Bottom-up *in-situ* Formation of Fe_3O_4 Nanocrystals in A Porous Carbon-Foam for Lithium-Ion Battery Anode Application

Taegyun Yoon[a], Changju Chae[a], Yang-Kook Sun[b], Xin Zhao[c], Harold H. Kung[c], Jung Kyoo Lee[a]*

[a]Department of Chemical Engineering, Dong-A University, Busan 604-714, Korea,
[b]Department of Energy Engineering, Hanyang University, Seoul 133-791, Korea,
[c]Department of Chemical and Biological Engineering, Northwestern University, Illinois 60208-312, USA

Supplementary Information

Energy-dispersive X-ray analysis of carbon foam (CF)

The removal of silica template (80nm, Nanostructured & Amorphous Materials Inc. USA) in the silica/carbon composite was examined by energy-dispersive X-ray analysis (EDX) measurement. The EDX spectra (Figure S1) examined on a large and a spot area on the CF revealed that the silica template was removed completely by HF etching followed by repeated DI washing.

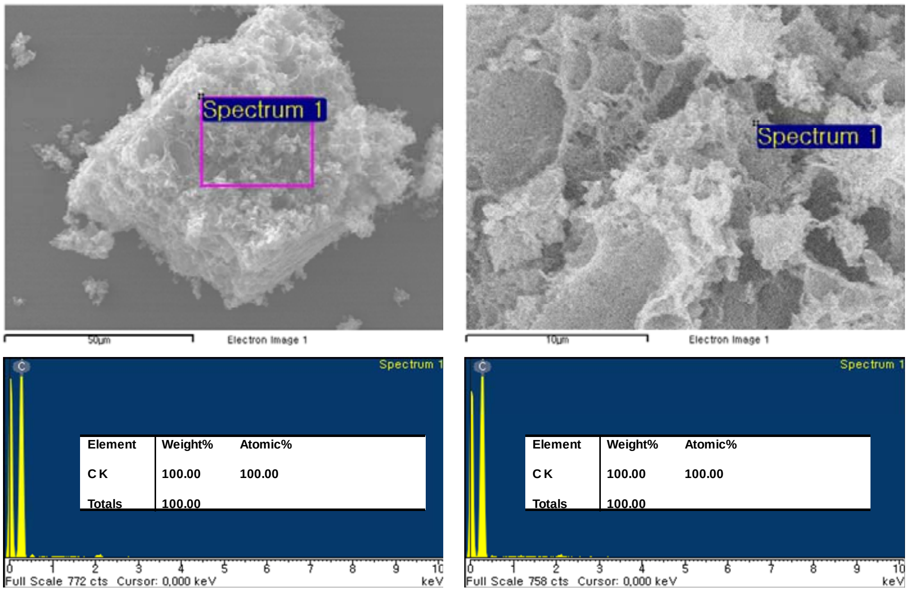

Element	Weight%	Atomic%
C K	100.00	100.00
Totals	100.00	

Element	Weight%	Atomic%
C K	100.00	100.00
Totals	100.00	

Figure S1. Energy-dispersive X-ray analysis of carbon foam. EDX scan on a large (left column) and a spot area on the carbon foam (right column), showing the complete removal of silica template by HF etching followed by repeated DI washing.

FE-SEM images of carbon foam (CF)

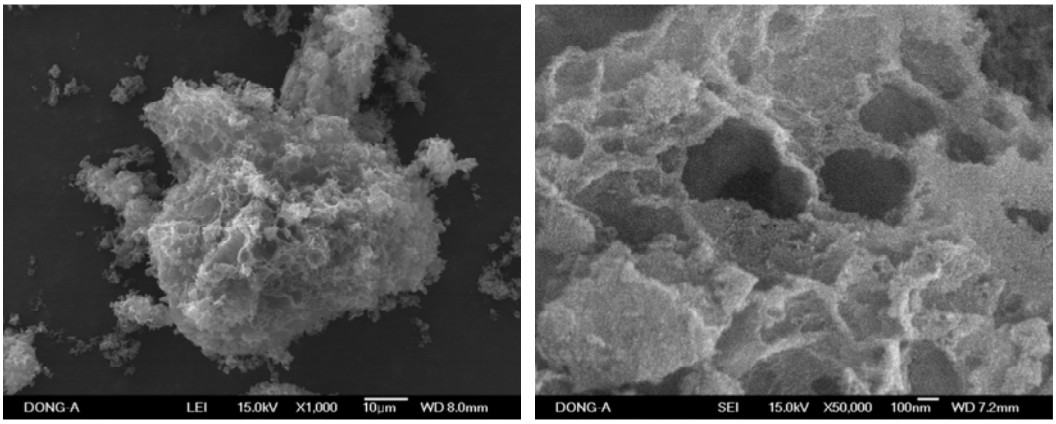

Figure S2. FE-SEM images of CF obtained at low (left) and high magnification (right). In the high magnification image, pores generated by silica nanoparticles of 80 nm can be observed together with large pores generated by aggregates of silica nanoparticles.

Magnetic property of Fe_3O_4/CF

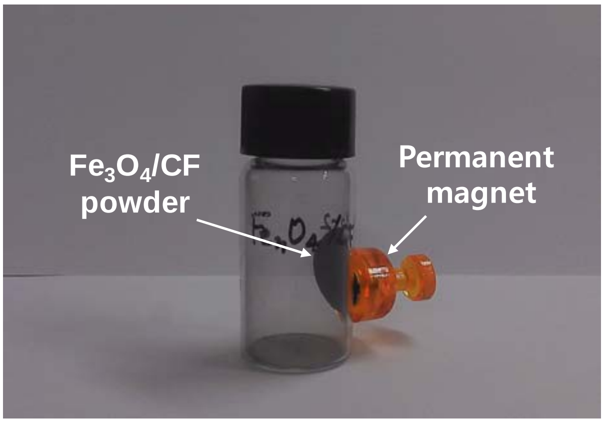

Figure S3. Photograph of Fe_3O_4/CF powder attached on a glass vial wall by a permanent magnet.

TEM image of Fe_3O_4/CF

In the Fe_3O_4/CF sample, some of large Fe_3O_4 nanocrystals formed on the surface of CF are observed as shown in Figure S4. From the TEM observation, about 10% of Fe_3O_4 nanocrystals are present on the external surface of CF. Better controlled impregnation of $Fe(NO_3)_3$ solution (impregnation of smaller portion of $Fe(NO_3)_3$ solution at a time) can prevent Fe_3O_4 nanocrystals formation on the external surface of CF thus can give more stable cycling performance of Fe_3O_4/CF.

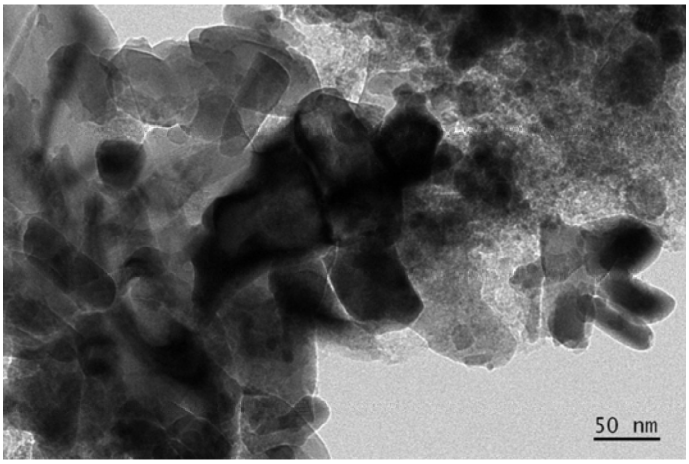

Figure S4. FE-SEM images of Fe_3O_4/CF showing large Fe_3O_4 nanocrystals formed on the external surface of CF.

XPS analysis of $Fe(NO_3)_3$/CF

To obtain surface chemical information of $Fe(NO_3)_3$/CF sample, XPS analysis was conducted and the spectrum is shown in Figure S5. The O1s peak at 530.71 eV is predominant in the sample and the N1s peak is observed at 405.55 eV. Fe shows two peaks at 710.3 and 724.5 eV, corresponding to trivalent $Fe_{2p3/2}$ and $Fe_{2p1/2}$, respectively (inset of Figure S5). From the peak area of O1s and from the area ratio of N1s to Fe2P3, Fe is present presumably in the form of $Fe(NO_3)x(OH)y \cdot zH_2O$ in the $Fe(NO_3)_3$/CF.

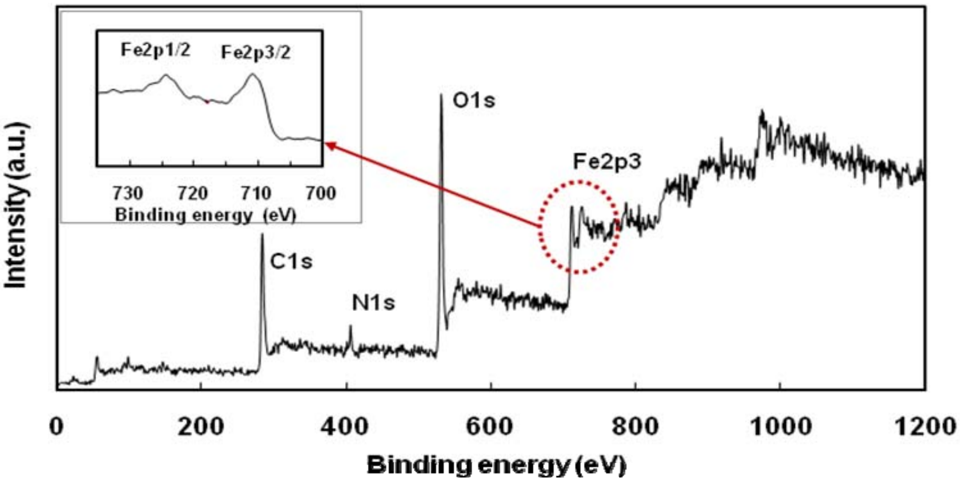

Figure S5. XPS spectrum obtained on the $Fe(NO_3)_3$/CF sample. Inset shows trivalent Fe2p3/2 and Fe2p1/2 peaks at 710.3 and 724.5 eV, respectively.

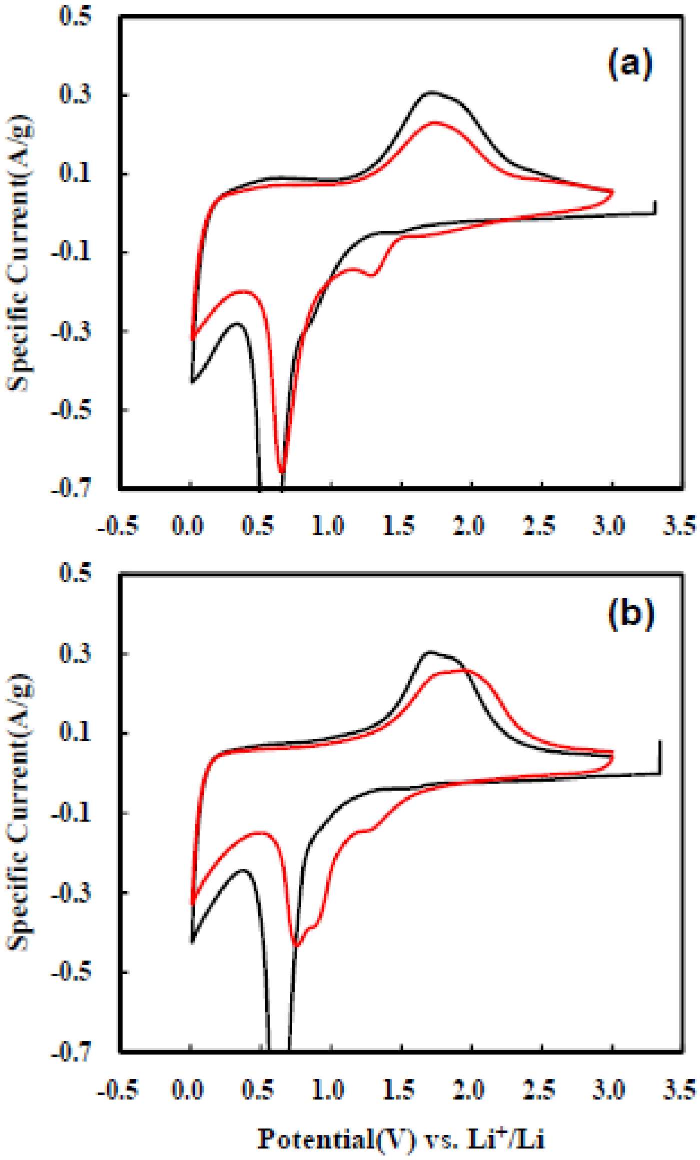

Figure S6. Cyclic voltammograms of (a) Fe_3O_4 nanocrystals and (b) Fe_3O_4/CF. Black line denotes for the 1st cycle and red line for the 2nd cycle.